

# Trends in Wind Speed at Wind Turbine Height of 80 m over the Contiguous United States Using the North American Regional Reanalysis (NARR)

ERIC HOLT AND JUN WANG

*Department of Earth and Atmospheric Sciences, University of Nebraska—Lincoln, Lincoln, Nebraska*

(Manuscript received 21 September 2011, in final form 4 June 2012)

## ABSTRACT

The trends in wind speed at a typical wind turbine hub height (80 m) are analyzed using the North American Regional Reanalysis (NARR) dataset for 1979–2009. A method, assuming the wind profile in the lower boundary layer as power-law functions of altitude, is developed to invert the power exponent (in the power-law equation) from the NARR data and to compute the following variables at 80 m that are needed for the estimation and interpretation of the trend in wind speed: air density, zonal wind  $u$ , meridional wind  $v$ , and wind speed. Statistically significant and positive annual trends are found to be predominant over the contiguous United States, with spring and winter being the two largest contributing seasons. Positive trends in surface wind speed are generally smaller than those at 80 m, with less spatial coverage, reflecting stronger increases in wind speed at altitudes above the 80-m level. Large and positive trends in winds over the southeastern region and high-mountain region are primarily due to the increasing trend in southerly wind, while the trends over the northern states (near the Canadian border) are primarily due to the increasing trend in westerly wind. Trends in the 90th percentile of the annual wind speed, a better indicator for the trend in wind power recourses, are 40%–50% larger than but geographically similar to the trends in the annual mean wind speed. The probable climatic drivers for change in wind speed and direction are discussed, and further studies are needed to evaluate the fidelity of wind speed and direction in the NARR.

## 1. Introduction

Fossil fuels provide almost 80% of the world's energy supply (Metz et al. 2007). In an effort to reduce the greenhouse gases emitted from the burning of fossil fuels, the last two decades have seen a rapid growth in harvesting wind power, an important form of renewable power. Between 1996 and 2010, the global installed wind power capacity increased from nearly 1280 MW to 35 802 MW (GWEC 2011). In the United States, the wind power-generating capacity has grown by an average of 29% per annum from 2003 to 2007 (AWEA 2009), and was reported as 1032 GW according to McElroy et al. (2009). Archer and Jacobson (2003), based upon surface observation data and radiosonde data, found that one-quarter of the United States may be suitable for providing electric power from wind at a direct cost equal to that of the costs required to extract new natural gas or

coal. While wind is often considered a sustainable power source, many recent studies based upon surface observations found a declining trend in surface wind speed over the last five decades in many parts of the world (as summarized in Table 1), including Australia (Roderick et al. 2007; McVicar et al. 2008), China (Xu et al. 2006a,b), Europe (Pirazzoli and Tomasin 2003), and North America (Klink 1999; Tuller 2004; Pryor et al. 2007; Hundecha et al. 2008). Over the United States, Pryor et al. (2009) found a  $0.84 \pm 0.32 \text{ m s}^{-1}$  decrease in the 90th-percentile 10-m winds from 1973 to 2005.

Admittedly, the declining trends of surface wind reported by previous studies generally are small ( $<0.1 \text{ m s}^{-1} \text{ yr}^{-1}$ ; Table 1) and hence are unlikely to interrupt the sustainability of wind energy resources, at least during the life span of a typical wind power plant (presumably 20–30 years) (Pryor and Barthelmie 2011). It is still important to assess the distribution of the trend in wind speed at the continental to global scale, however, to better understand the causes of the trend as well as to develop wind farms strategically and economically (Pryor et al. 2009; Griffin et al. 2010). This is especially true in the continental United States, where wind farms

---

*Corresponding author address:* Jun Wang, University of Nebraska—Lincoln, Dept. of Earth and Atmospheric Sciences, 303 Bessey Hall, Lincoln, NE 68588.  
E-mail: jwang7@unl.edu

TABLE 1. Summary of previous work showing the declining trend in near-surface wind speed.

Location	Time span	No. of sites	Trend ( $\text{m s}^{-1} \text{ yr}^{-1}$ )	Height <sup>a</sup> (m)	Reference
Australia	1975–2006	163	−0.009	Station data: 2; model data: 10	McVicar et al. (2008)
Australia	1975–2004	41	−0.01	2	Roderick et al. (2007)
United States	1960–90	176	−0.004	6–21	Klink (1999)
United States	1973–2005 <sup>b</sup>	193	−0.026	10	Pryor et al. (2009)
China	1960–2000	150	−0.008	10	Xu et al. (2006a)
China	1969–2000	305	−0.2	10	Xu et al. (2006b)
Loess Plateau, China	1980–2000	52	−0.01	10	McVicar et al. (2005)
Italy	1955–96	17	−0.013	Unavailable	Pirazzoli and Tomasin (2003)
Canada	1979–2004	13	Variable	10	Hundecha et al. (2008)
Canada	1950–95 <sup>c</sup>	4	−0.017	3–92	Tuller (2004)

<sup>a</sup> The altitude at which the wind speed is measured or analyzed.

<sup>b</sup> Period of record includes 1979–2000.

<sup>c</sup> Years are approximate; each station has a different period of record.

(triangles in Fig. 1) have undergone rapid commercial development (Foltz et al. 2007) and carry a potential to accommodate up to 16 times the current U.S. demand for electricity (Lu et al. 2009).

Previous assessments of surface wind speed *trend* over the continental United States were conducted by Klink (1999) for 1961–90 and more recently by Pryor et al. (2009) for 1973–2005, with ground-based observations. Pryor et al. (2009) noted, however, that the ground-based

observations, despite their accuracy, are not sufficient to provide a coherent analysis of the distribution of the trend in wind speed at the continental scale because of the limited spatial coverage, temporal discontinuity, and heterogeneity in the wind measurements. Another limitation involves inconsistent altitudes (ranging from 2 to 30 m; Table 1) at which wind speeds were measured. Furthermore, it was found that tree growth around surface stations can explain between 25% and 60% of

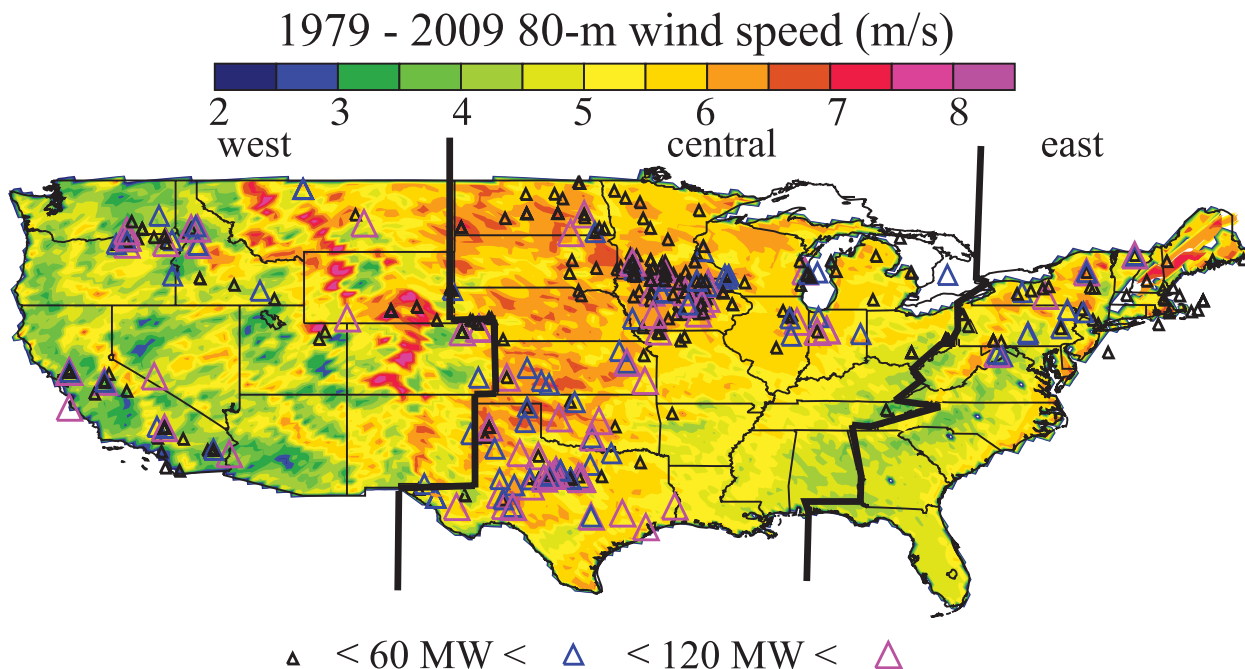


FIG. 1. Mean of annually averaged 80-m wind speeds ( $\text{m s}^{-1}$ ) for 1979–2009. The 80-m wind speeds are estimated assuming the wind profile in the boundary layer as the power-law distribution [Eq. (5)], and their annual averages are computed from their monthly averages. Triangles represent the location of all U.S. wind farms (as of 31 Dec 2009), with their size being proportional to the farms’ power capacity (kW). Also shown are the western, central, and eastern regions of the contiguous United States, as defined in this study for the regional analysis of wind power.

the observed surface wind trend decrease from 1979 to 2008 over many stations around the globe (Vautard et al. 2010).

In contrast, the use of model-based data, given the uncertainties and occasional errors in the model, allows for the analysis of wind speed at a continental scale to be amenable to the physics of that model, which consequently can help with the interpretation of regional trends (if any) from a synoptic point of view. To evaluate the trends in wind speed, many recent studies have used a meteorological reanalysis dataset, which is an optimal combination of model data and observational data (McVicar et al. 2008; Pryor et al. 2009; Li et al. 2010; Vautard et al. 2010). In addition to the negative trends found in the ground-based observation record, Pryor et al. (2009) also showed the dominance of positive trends in the National Centers for Environmental Prediction–National Center for Atmospheric Research (NCEP–NCAR) reanalysis and the 40-yr European Centre for Medium-Range Weather Forecasts (ECMWF) Re-Analysis (ERA-40) for the 50th-percentile and 90th-percentile annual mean wind speed and further found that wind speed trends at 0000 and 1200 UTC from the North American Regional Reanalysis (NARR) are opposite in sign over the west. Overall, past studies support the synthesis by Pryor et al. (2009) that the surface wind speeds over the continental United States exhibit different and sometimes opposite trends depending on the dataset used, the time period examined, and the region of interest (Pryor et al. 2007; McVicar et al. 2008; Pryor et al. 2009; Li et al. 2010; Griffin et al. 2010).

While the implication of the trend in surface wind speed has often been interpreted in the context of the development of wind energy (in many aforementioned studies), it is at 80 m above the surface (i.e., a typical height for a wind turbine) where wind energy is harvested. Given that wind speed generally increases (nonlinearly) with altitude in the planetary boundary layer (Arya 2001), the trend in surface wind that is estimated or measured at either 8 or 10 m above the surface may not be representative of the trend in wind speed at 80 m. Indeed, in contrast to the widely reported decline in surface wind speed (see references in last three paragraphs), Vautard et al. (2010) found an increase in wind speed in the lower-to-midtroposphere using radiosonde data. Furthermore, because wind power is proportional to the third power of wind speed at 80 m (if neglecting friction and other mechanical losses), the trend in wind speed at 80 m, while expected to have the same sign, may have different values (and statistical significance) than the trend in wind power potential. Hence, further studies are needed to reveal the link between the trend in wind speed at the surface

and the respective trends for the wind speed at 80 m and its cube at that same height.

In this study, we explore the trends in wind speed at 80 m above the surface over the continental United States using the NARR data from 1979 to 2009. Our analysis differs from past studies in that we 1) focus on the trend in the wind speed at a typical wind turbine hub height [80 m; Ray et al. (2006)], 2) include estimates of the trends for zonal and meridional wind speed at 80 m, and 3) discuss the likely climate drivers for any trends we find. The assessment of the trend in wind speed in the zonal and meridional directions is important, because this knowledge is lacking from past studies and is necessary to explain and/or hypothesize the likely cause for climatic change in wind speed. We describe the NARR data and our analysis method in sections 2 and 3, respectively; present the results and their interpretation in sections 4 and 5, respectively; discuss the implication of this study for the trend in wind power potential in section 6; and summarize the paper in section 7.

## 2. NARR data

The primary dataset used for this analysis is the NARR dataset, which is archived at the National Climatic Data Center. The NARR data are derived from the NCEP–U.S. Department of Energy (DOE) Global Reanalysis, the NCEP regional Eta Model and its data assimilation system, and a version of the “Noah” land surface model (Mesinger et al. 2006). The dataset has 45 vertical layers with a horizontal grid spacing of approximately  $32 \text{ km} \times 32 \text{ km}$  over the continent of North America. The NARR has a vertical grid spacing of 25 hPa ( $\sim 200 \text{ m}$ ) from 1000 to 800 hPa, which is arguably more coarse than what is needed for a detailed representation of the vertical atmospheric structure but still is among the available climate datasets with finest resolution for studying wind power, especially considering that the NARR dataset spans from 1979 to the present, every 3 h (0000–2100 UTC) with assimilation using the Regional Climate Data Assimilation System (R-CDAS; Ebisuzaki et al. 2004). Extensive tests to assess the impact of assimilating surface observations found that the 10-m winds and 2-m temperatures in the NARR dataset are improved relative to the NCEP–DOE Global Reanalysis dataset (Mesinger et al. 2006). The boundary layer scheme for the NARR or in the NCEP Eta Model is based upon the Mellor–Yamada turbulence closure scheme (Mellor and Yamada 1974), but with refinement in the parameterization (of length scale) and an improvement in the handling of reliability (Janjić 1994). Mesinger (2010) summarized the progress of the Eta Model’s output after various recent refinements

in the boundary layer scheme and the assimilation of wind data from surface observations and rawinsondes, and found improved accuracy in wind speed in the NARR dataset (when compared with the NCEP–NCAR reanalysis).

Of particular interest to this study is the NARR-reported wind speeds at 10 and 30 m (Mesinger et al. 2006). As pointed out by Pryor et al. (2009) and NCEP (<http://www.emc.ncep.noaa.gov/mmb/rreanl/faq.html>), both wind speeds are extrapolated on the basis of mid-layer winds at the four neighboring mass points at the lowest of 45 model layers following a procedure originally developed by Loboeki (1993) and described in detail by Chuang et al. (2001). Since a minor error is found in the code for the calculation of 30-m wind speed, which results in zero values in high terrain and coastal regions (<http://www.emc.ncep.noaa.gov/mmb/rreanl/faq.html#zero-30m-winds>), 30-m wind speed is disregarded in the analysis of this study. Mesinger et al. (2006) evaluated the 10-m wind speed in the NARR over the 450 meteorological stations across the continental United States for January 1988 and July 1988 and found a low bias within  $1 \text{ m s}^{-1}$  on daily average. While the NARR 10-m wind data have also been used in Li et al. (2010) and Pryor et al. (2009), respectively, for studying the trend in 80-m wind speed in the Great Lake regions and surface wind trend over the continental United States, the question about the link between trends in surface wind speed and wind speed at 80 m in the NARR still remains.

### 3. Methods

#### *a. Method for estimating the 80-m wind vector*

We derive 80-m winds every 3 h from the corresponding 10-m and level-based wind data from 1979 to 2009. At each model grid and time, our method is to first find two vertical layers from all model layers (including the 10-m layer) in the NARR that bracket the 80-m altitude and then to estimate the wind speed at 80 m through interpolation on the basis of the wind speeds in these two layers. We argue that extrapolation or interpolation of the wind at turbine height is usually necessary because neither measured nor modeled wind data are common at 80 m (Peterson and Hennessey 1978; Archer and Jacobson 2005; also Table 1).

To be specific, we first find the model pressure level that is closest to and above the target height and denote this level as  $P_1$ . With the NARR's fine vertical resolution (25 hPa or 200 m) near the surface, the geometric thickness from the surface to  $P_1$  can be computed with the hydrostatic equation:

$$\Delta h_1 = \frac{\Delta P}{\rho g} = \frac{P_{\text{sfc}} - P_1}{\rho g}, \quad (1)$$

where  $\Delta P$  is a difference in pressure (Pa),  $P_{\text{sfc}}$  is surface pressure,  $\rho$  is air density ( $\text{g m}^{-3}$ ), and  $g$  denotes the gravitational acceleration rate ( $9.81 \text{ m s}^{-2}$ ). Note that  $\rho$  varies with elevation and moisture content in the air and that such variability is taken into account in our calculations.

If the thickness  $\Delta h_1$  is larger than 80 m, then the wind speeds at 10 m and at the pressure level  $P_1$  will be used in the interpolation to estimate the wind speed at 80 m. Otherwise, we will compute the thickness  $\Delta h_2$  between  $P_1$  and the pressure level right above  $P_1$  (hereinafter  $P_2$ ). Because the vertical gridpoint spacing of the NARR is equal to or larger than 25 hPa,  $\Delta h_2$  is usually larger than 80 m, which makes  $P_2$  the model pressure level right above the altitude of 80 m from the surface. In cases in which  $\Delta h_1$  is less than 80 m (which can be true depending on surface pressure), we will use the wind speed between  $P_1$  and  $P_2$  for the interpolation at 80 m. With the method above, we can identify the two closest model levels that bracket the 80-m height and can infer the height of both levels above the surface (hereinafter  $Z_{\text{b80}}$  and  $Z_{\text{a80}}$ ).

To use winds speeds ( $V_{\text{b80}}$  and  $V_{\text{a80}}$ , respectively) at altitudes of  $Z_{\text{b80}}$  and  $Z_{\text{a80}}$  for estimating winds at 80 m requires an assumption about the variation of wind speed with height (i.e., a wind profile). Two types of wind profiles are commonly used in the literature. One is the logarithmic profile that describes the wind speed at altitude  $Z$  as

$$V_Z = V_{\text{a80}} \frac{\ln(Z/z_0)}{\ln(Z_{\text{a80}}/z_0)}, \quad (2)$$

where  $z_0$  is surface roughness. While Eq. (2) is widely used in estimating the change in wind speed in the boundary layer according to the recent literature (Robeson and Shein 1997; Archer and Jacobson 2005; Klink 2007; Capps and Zender 2009), it is expected to have higher accuracy over the surface in areas with low canopy height and when the surface layer is neutral (Arya 2001). Over surfaces that are covered by tall trees or buildings, the displacement height must be subtracted from the altitude  $Z$  in Eq. (2); the displacement height is smaller than but close to the height of the surface canopy (i.e., trees or buildings) and is the height at which the wind speed is zero (Arya 2001). Since Eq. (2), without consideration of displacement height, gives a zero wind speed at surface roughness  $z_0$  that is  $\sim 0.1$ – $0.2$  of the displacement height, it may yield a significant overestimation of wind speed over areas with tall trees or buildings.

Another commonly used profile is the power-law profile (Robeson and Shein 1997; Elliot et al. 1986; Arya 2001; Archer and Jacobson 2003):

$$V_Z = V_{a80} \left( \frac{Z_{a80}}{Z} \right)^\alpha, \quad (3)$$

where the exponent  $\alpha$  is the friction coefficient and generally increases with roughness length  $z_0$ . In comparison with the logarithmic profile, which has a more sound physical basis and appears to be valid within the neutral surface layer, the power-law profile essentially is an empirical formula and can be a good fit to the logarithmic profile when the surface layer is neutral and  $Z$  does not deviate significantly from the reference height [here  $Z_{a80}$  in Eqs. (2) and (3); Arya (2001)]. As argued by Archer and Jacobson (2003), however, the surface layer is seldom neutral, and their analysis of rawinsonde data collected at 80 stations during 2000 showed that Eqs. (2) and (3) on average underestimate the wind speed at 80 m by 1.7 and 1.3  $\text{m s}^{-1}$ , respectively. Given that Eq. (3) has similar (if not slightly better) accuracy in comparison with Eq. (2), it is used in this study to be consistent with previous studies of trend analysis (Pryor and Barthelmie 2011). To reduce the uncertainties in the future estimation of 80 m from the use of either the power-law profile or the log profile, we recommended that numerical models add a vertical layer as close as possible to 80 m and then archive it in the reanalysis.

Although this study assumes a power-law profile that is similar to those used in many previous studies, our approach of using Eq. (3) is different in that we consider the variation of  $\alpha$  due to the change of surface roughness or atmospheric stability (Arya 2001). A constant value of  $\alpha$  ( $=1/7$ ) has been used in the development of the Wind Resource Map at the National Resource Energy Laboratory (NREL) as well as in a recent model-based assessment of future wind energy trends (Pryor and Barthelmie 2011). Applying Eq. (3) to 80 m and selecting  $Z_{b80}$  and  $Z_{a80}$  as the reference heights, we can derive

$$\alpha = \frac{\ln \frac{V_{b80}}{V_{a80}}}{\ln \frac{Z_{b80}}{Z_{a80}}} \quad (4)$$

and

$$V_{80} = V_{b80} (80/Z_{b80})^\alpha. \quad (5)$$

On the basis of Eqs. (4) and (5), the 80-m wind  $V_{80}$  can be derived. As shown in section 4a, this approach yields

results that are more reasonable than using a constant  $\alpha$  ( $=1/7$ ).

After the wind speed at 80 m is calculated, the next step is to estimate the  $u$  and  $v$  components at 80 m (hereinafter  $u_{80}$  and  $v_{80}$ , respectively). We derive the wind directions  $\gamma$  at two different levels below and above 80 m, and the wind direction  $\gamma_{80}$  at 80 m is computed under the assumption that wind direction varies linearly as a function of altitude. In the numerical realization of this method, the value of the wind direction is defined as 0 for westerly wind and  $3\pi/2$  for northerly wind. The sequential change in wind directions at  $Z_{b80}$ , 80 m, and  $Z_{a80}$  is ensured to be no larger than  $\pi$  as we assume that the wind shear cannot be larger than  $\pi$  within the NARR's vertical resolution (25 hPa, or 120 m). Regardless of any backing or veering that may be taking place at a given point, this assumption results in the smallest (and also often sequential and continuous) change in wind direction as the altitude changes from  $Z_{b80}$  to 80 m or from 80 m to  $Z_{a80}$ . This assumption certainly is not always true, and Arya (2001) showed a case in which a  $180^\circ$  change in wind direction is observed in as little as 32 m, but such cases are presumably rare.

After the wind direction at 80 m is correctly computed, the  $u$  and  $v$  components at 80 m are estimated as  $u_{80} = V_{80} \cos(\gamma_{80})$  and  $v_{80} = V_{80} \sin(\gamma_{80})$ . Figure 2 presents sample wind profiles at two different locations to illustrate the accountability for the varying topography (and hence surface pressure) in our methods of using power-law and linear interpolation to estimate winds at 80 m. In Fig. 2a, the surface pressure is 1014 hPa, and our method is able to find the model pressure level right above 80 m, which is 1000 hPa. In Fig. 2b, for which the surface pressure is 992 hPa, our method is able to correctly find the pressure level right above 80 m as 975 hPa. Hence, depending on local terrain/pressure variations, either the surface pressure or a pressure level within the NARR is used as the base level for interpolation. Both Figs. 2a and 2b indicate that the location and magnitude of the calculated  $u_{80}$ ,  $v_{80}$ , and total wind speed at 80 m above the surface are consistent with the NARR wind profile.

#### b. Method for analysis of wind trend

The trends in wind (at each grid point) from 1979 to 2009 are investigated using linear regression [i.e., ordinary least squares methods (OLS)] after correction of temporal autocorrelation in the time series. Only the linear trends at the 90% significance level or higher are considered to be statistically significant [similar to what is used in Pryor et al. (2009)], using a two-tailed  $t$  test for each grid point. OLS is widely used in the

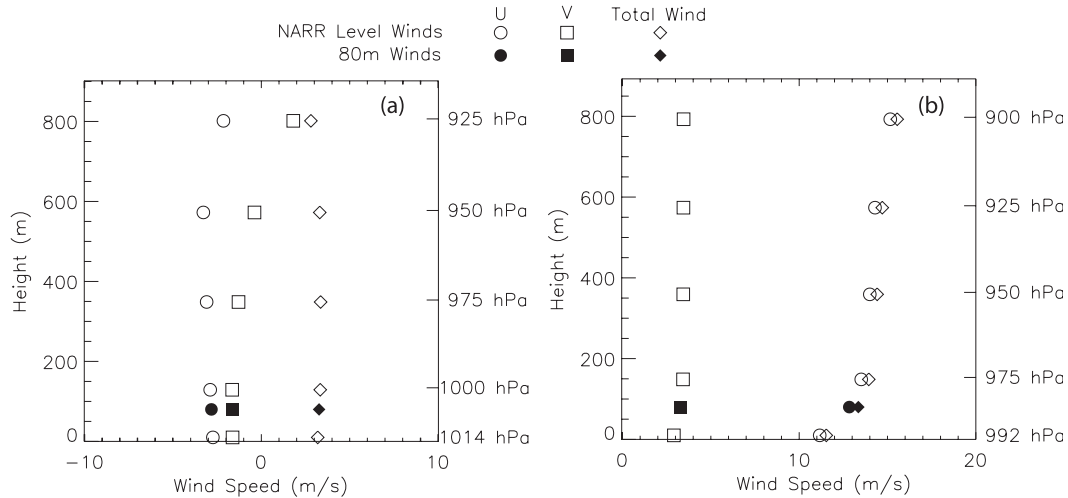


FIG. 2. (a) Vertical profile for winds at different NARR levels and the winds estimated at 80 m above the surface on 0000 UTC 1 Jan 1979 at 35.13°N, 98.10°W. Shown are NARR pressure levels and surface pressure (hPa) on the right y axis and the corresponding estimated height above the surface (m) on the left y axis. (b) As in (a), but for 31.98°N, 111.05°W to illustrate the accountability for the varying topography (and hence surface pressure) in our methods of estimating wind at 80 m (see section 3a for details).

analysis of wind trend (McVicar et al. 2008; Pryor et al. 2009; Li et al. 2010), but Pryor and Ledolter (2010) and Griffin et al. (2010) recently noted that significant temporal autocorrelation of wind may occur in a time span of 30 years, depending on the geographical location, and must be filtered out of the time series before applying OLS; otherwise, the temporal autocorrelation may exaggerate the statistical significance of the trend.

Development of an ideal method to remove the temporal autocorrelation in the time series is practically challenging because the mechanisms that govern the interannual and intraannual variability of wind speed are not well known (Pryor and Barthelmie 2011). Nevertheless, the Durbin–Watson (DW) test (Wilks 2006) is used here to test the statistical significance of temporal autocorrelation, and the Cochrane–Orcutt (CO) method described in Thejll and Schmith (2005) is used to correct any significant temporal autocorrelation in the time series of wind data at each model grid. In brief, consider a linear regression model for the time series of wind speed  $V$ :

$$V_t = a + Rt + \delta_t, \tag{6}$$

where  $t$  represents time (in unit of months or years in this study),  $R$  and  $a$  are slope and intercept, respectively, and  $\delta_t$  is the residual term. In the CO method as described in Thejll and Schmith (2005), the first-order autoregression model is used to simulate  $\delta_t$ :

$$\delta_t = r\delta_{t-1} + \varepsilon_t, \tag{7}$$

where  $r$  is lag-1 autocorrelation correlation and  $\varepsilon$  is a serially independent number with a mean of zero and constant variance. Hence, with the CO method, the key is to find  $r$  so that 1) the DW distance of the resultant  $\delta$  [or the residual in Eq. (6)] is larger than a critical value needed to ensure that the null hypothesis of no temporal correlation in  $\delta$  cannot be rejected (Wilks 2006) and 2) the resultant Eq. (6) can be statistically significant with the OLS method. As recommended in Thejll and Schmith (2005),  $r$  can be first started with some initial values, and then  $r$  and the pair of  $a$  and  $R$  are computed iteratively using Eqs. (6) and (7) (within the framework of the OLS approach) until their values converge. Failure to meet conditions 1 and 2 indicates that there is no significant linear trend in the wind speed.

From a statistic point of view, we found that 80% of the time series of wind speed data analyzed in this study need the correction of temporal autocorrelation. After using the CO method to remedy the effect of the temporal autocorrelation, the significance of trends in most time series is lowered, but often by less than 5%. This result is similar to that of Pryor and Ledolter (2010), who showed that “treatment of temporal autocorrelation slightly reduces the number of stations for which the linear trends in 10-m wind speed are deemed significant (at the 90% confidence level),” and the magnitudes of the wind speed trends reported using OLR may also be relatively insensitive to (untreated) temporal autocorrelation. Examples showing the statistics computed from linear regression with the OC method

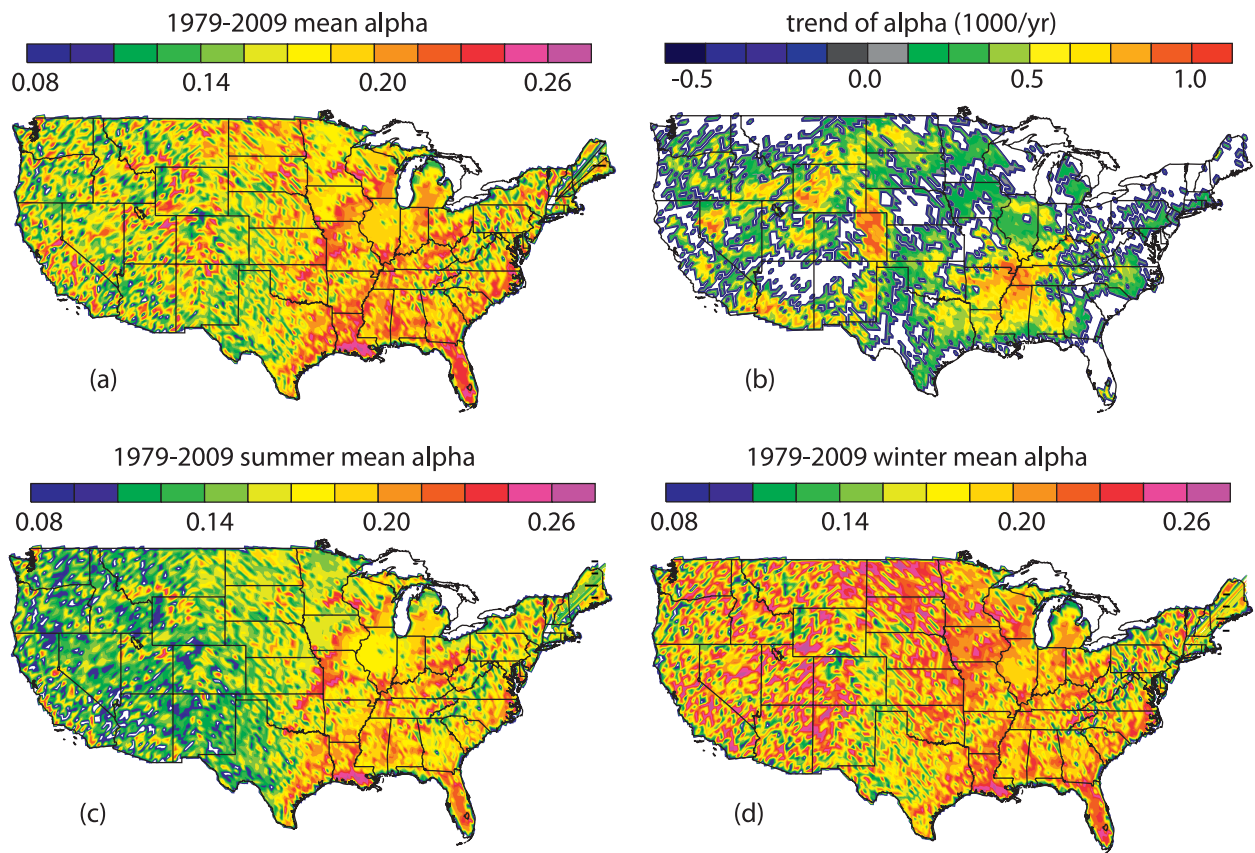


FIG. 3. (a) Geographical distribution of the mean of the 1979–2009 annual averages of  $\alpha$ , the exponent used in the power-law equation for deriving wind at 80 m and computed from Eq. (4) in the text. (b) Geographic distribution of the trend in annually averaged  $\alpha$ . Areas in white indicate the regions that either are covered by a water surface or have statistically insignificant trends. (c),(d) As in (a), but for the mean during summer and winter, respectively, during 1979–2009.

are shown in Fig. 6 (described later) and are discussed in section 4e.

#### 4. Results

##### a. Geographical distribution of the wind and power exponent $\alpha$ climatology

Figure 1 shows the 30-yr normal (“climatology”) of annually averaged 80-m wind speed throughout the contiguous United States. Larger values ( $\sim 7\text{--}8\text{ m s}^{-1}$ ) are evident over the Dakotas, Minnesota, and Nebraska, with lower values ( $3\text{--}4\text{ m s}^{-1}$ ) over the coastal regions. Higher values of wind power generally indicate the regions with the most potential for commercial development, which has been the case, as shown in Fig. 1. Topographic effects on the wind are evident over the mountainous western regions, as well as the Appalachian Mountains region.

As discussed in section 3a, past methods for estimating the wind speed at 80 m above the surface have

assumed a constant value for the power exponent [i.e.,  $\alpha$  in Eqs. (2) and (3)] of either  $1/7$  [ $\sim 0.14$ ; Pryor and Barthelmie (2011)] or 1 [i.e., linear interpolation; Li et al. (2010)] regardless of season and geographical location. For comparison, Fig. 3a shows the map of the 1979–2009 climatology of  $\alpha$  as estimated using the method [Eq. (4)] in this study. A remarkable finding is that  $\alpha$  values over the majority of the United States are in the range of 0.16–0.20 and, thus, are consistent with the value of 0.17 used by NREL, as well as in Pryor and Barthelmie (2011). As summarized by Arya (2001), however, the exponent  $\alpha$  usually changes with time and space and increases with both surface roughness and boundary layer stability. In the NARR, the surface roughness length does not change with time and is set to 0.1 plus the correction for topography (Pryor et al. 2009). Nevertheless, we argue that our method of using wind speeds at two vertically adjacent layers to invert (recover) power exponent  $\alpha$  (which is not saved in the NARR) has its advantage (over past methods), because the atmospheric stability and orographic effects have been

considered in the NARR's boundary layer scheme to estimate the winds near the surface (Mellor and Yamada 1974; Loboeki 1993; Janjić 1994). These advantages should be illustrated best by using daily or weekly data, but they are still partially reflected in the climatology in Fig. 3a where larger  $\alpha$  values are found in the U.S. western and southeastern mountainous regions, reflecting the impact of topography on the wind profile. Furthermore, the contrast of the calculated climatology of  $\alpha$  values in the summer and winter, as shown in Figs. 3c and 3d, also manifests the effect of lower-atmospheric stability. For instance, a more stable boundary layer during the winter over the western and central United States generally results in a larger  $\alpha$  (as shown in Fig. 3d) for these regions (Arya 2001). The growth of the canopy (leading to larger  $\alpha$  values) and the decrease in atmospheric stability (leading to smaller  $\alpha$  values) in the summer over the eastern United States may counteract each other, which would lead to a smaller change in  $\alpha$  values between the summer and the winter (cf. Figs. 3c and 3d).

#### b. Geographical distribution of trends of friction coefficient $\alpha$

Vautard et al. (2010) attributed the decline in the measurements of surface wind to the increase in surface roughness. The database of surface roughness is generally prescribed in the weather models, however, and hence is unlikely to explain any trend in wind speed we may find from the NARR. For curiosity, we show the trend in the friction coefficient  $\alpha$  in Fig. 3b, indicating an increase in  $\alpha$  over most of the contiguous United States, with larger trends in the Southeast, high plains, and Intermountain West regions. Note that the trend values shown in Fig. 3b have been multiplied by 1000. A 15%–20% increase in  $\alpha$  can be found over the Southeast and the high plains over the course of 31 years.

Interpretation of the increase in  $\alpha$  needs further investigation, but it could be related to the change in atmospheric stability [as theoretically modeled in Barthelmie (1999)], the increase (decrease) of wind above (below) 80 m, or a combination thereof. It is thus expected that, in regions where  $\alpha$  increases, a smaller increasing trend in surface wind may lead to a disproportionately larger increasing trend in the wind speed at 80 m [Eq. (5)], which is indeed the case, as shown in section 4c.

#### c. Geographical distribution of trends in annually averaged wind

Our calculations indicate a consistent positive trend [ $\sim 0.15 \text{ m s}^{-1} (10 \text{ yr})^{-1}$ ] of 10-m wind speed over many parts of the contiguous United States during 1979–2009

(Fig. 4a). Trends of up to  $0.3 \text{ m s}^{-1} (10 \text{ yr})^{-1}$  for 10-m wind speed are found in areas of the central plains and upper Midwest. From a geographic perspective, these positive trends are consistent with the time-truncated analysis of the 90th percentile of 10-m wind trends in the 1979–2006 NCEP global reanalysis dataset at both 0000 and 1200 UTC and in the NARR data at 0000 UTC (Pryor et al. 2009), especially over the Midwest.

Trends in 80-m wind (Fig. 4b) are more positive [usually larger than  $0.1 \text{ m s}^{-1} (10 \text{ yr})^{-1}$ ] than their counterparts at 10 m. Since topography generates more mechanical turbulence and shear in the mountainous regions, trends in 10-m wind are more representative of those at 80 m, which explains the relatively smaller differences between Figs. 4a and 4b over the mountain regions. Conversely, over flatter regions such as the Great Plains, 80-m winds are more influenced by winds higher in the boundary layer and the free atmosphere, explaining some of the large differences in trends between 10 and 80 m. Winds at 80 m (Fig. 4b) have shown increases of up to  $0.25 \text{ m s}^{-1} (10 \text{ yr})^{-1}$  for low-topographic areas, with little (if any statistically) discernible areas of declining trends. Consistent with Li et al. (2010), we found a positive but slightly larger trend over the Great Lakes region, likely reflecting the wind profile difference [i.e., the power law in this study vs linear interpolation in Li et al. (2010)] in the estimates of 80-m wind. The regions containing the more-positive trends are the Midwest; eastern Colorado and New Mexico; Montana and North Dakota; and parts of Appalachia.

The positive trends in  $u$  and  $v$  wind speed at 80 m over the United States (Figs. 4c and 4d) showed that over the southeastern United States the trend in  $v$  wind is much stronger than that of  $u$ , suggesting the possibility of a stronger low-level jet from the Gulf of Mexico to the Great Plains. In a similar way, the increasing trend in wind in the northern states (close to the border with Canada) is more due to the change of  $u$ , possibly indicative of changes in the midlatitude jet. An investigation of these possibilities requires a seasonal trend analysis of the wind speeds in different directions.

#### d. Seasonal trends

Figure 5 shows the trends for the seasonal averages of westerly, easterly, northerly, and southerly winds at 80 m for the following four seasons: winter (December–February), spring (March–May), summer (June–August), and autumn (September–November). One consistent feature we see in Fig. 5 is the generally larger positive trends in westerly and southerly winds during all seasons, which is not found with the easterly and northerly winds.

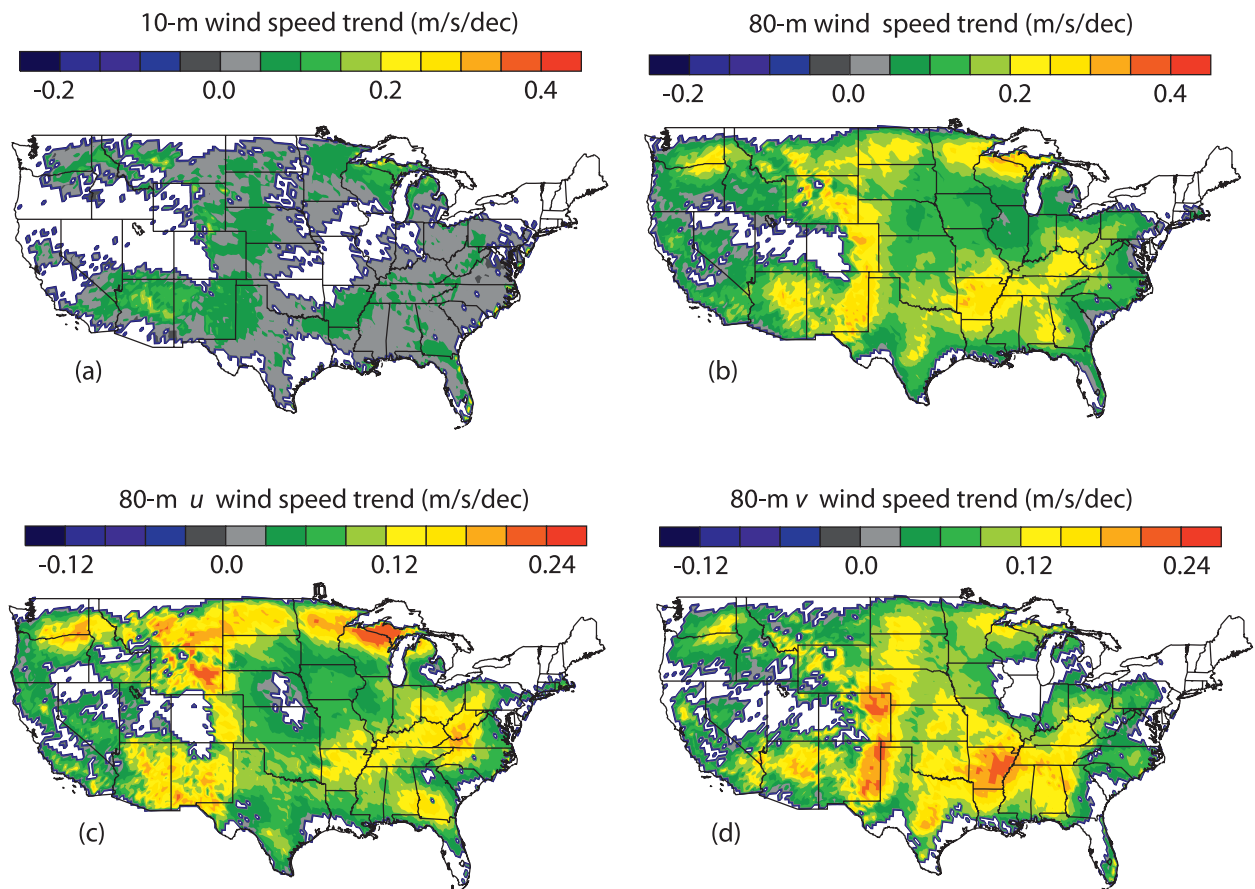


FIG. 4. (a) Geographical distribution of linear trends [ $\text{m s}^{-1} (10 \text{ yr})^{-1}$ ] for annually averaged 10-m wind speed from 1979 to 2009. (b)–(d) As in (a), but for the trends of 80-m wind speed, 80-m zonal ( $u$ ) wind speed, and 80-m meridional ( $v$ ) wind speed, respectively. Shaded regions indicate that the trends are at the 90% significance level or higher. Areas in white indicate that the regions either are covered by a water surface or have statistically insignificant trends.

In geographic terms, positive trends as large as  $\sim 0.24 \text{ m s}^{-1} (10 \text{ yr})^{-1}$  are found for the westerly wind in all seasons over states from the west to the Great Lakes near the border with Canada (Figs. 5a, 5e, 5i, and 5m), and similar magnitudes of the trends for the southerly wind are consistently found over the western part of the high plains region of eastern Colorado, New Mexico, and parts of the Dakotas, Nebraska, and Minnesota (Figs. 5c, 5g, 5k, and 5o). In winter and spring, the southerly wind shows a consistently large trend over the southeastern part of the United States. In contrast, larger trends for easterly wind are found over the Great Lakes region in all seasons except autumn (Fig. 5n). For northerly wind, larger trends are found over Arizona during winter and autumn, northern California in autumn, and the Nebraska panhandle region in spring. The lower Mississippi River valley has similar trends during the spring, summer, and autumn (Figs. 5h, 5l, and 5p). No significant trends are found

over the New England region and Florida for all seasons.

Overall, comparison between Fig. 5 and Figs. 4b and 4c reveals that the large trends in annual wind speeds and zonal wind speeds in the northern border states are primarily influenced by the westerly wind in all seasons (except in spring and summer when the easterly wind also plays an equal role in Minnesota and North Dakota). The large trends in annual wind speed and meridional wind speeds in the high plains regions of eastern New Mexico, Colorado, and Wyoming; western Nebraska; and Kansas are primarily affected by the trends in southerly wind during all seasons. The large trends in annual wind speed over the southeastern United States are driven both by westerly and southerly winds during the spring and winter and by the westerly, easterly, and northerly winds during autumn. In terms of seasons, spring and winter are the two seasons that contribute the most to the annual trend, whereas the summer contributes the least. The summer

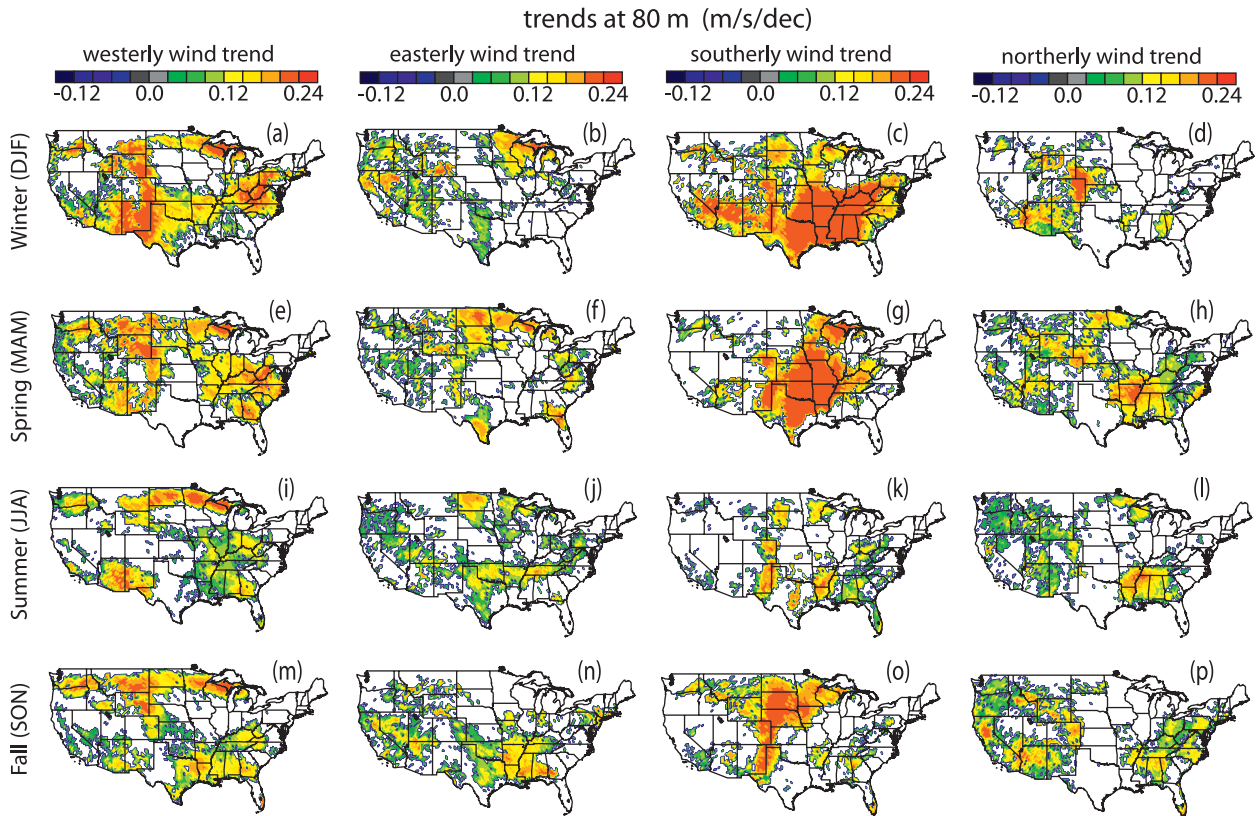


FIG. 5. Geographical distribution of linear trends [ $\text{m s}^{-1} (10 \text{ yr})^{-1}$ ], respectively, for seasonal averages of 80-m (left) westerly, (left center) easterly, (right center) southerly, and (right) northerly wind during (top) winter, (top middle) spring, (bottom middle) summer, and (bottom) autumn for 1979–2009. Areas in white indicate that the regions either are covered by a water surface or have statistically insignificant trends.

season does significantly influence the annual  $u$  and  $v$  component trends over the Midwest and parts of the high plains, however, with the  $v$  (both northerly and southerly) component trends generally being larger than the  $u$  (easterly and westerly) component trends. The autumn season also influences the annually averaged trends, but only significantly so over the Dakotas and Minnesota. The region with the most consistent positive trends for zonal and meridional wind speed in all seasons is the high plains region of eastern New Mexico, Colorado, and Wyoming, in which the trend in the southerly wind component is the primary contributor. Over the Great Lakes region and the northern border states, the trends in westerly wind are the primary contributor. Both regions contain the most consistent wind power source and should be recommended as a prime area for future commercial wind power development (if disregarding other factors such as transmission-line limitations and environmental impacts in those regions).

#### e. Regional trend

After investigating the annual and seasonal trends for every grid point over the contiguous United States,

trends in annual mean wind and wind power are analyzed by region. Grid points for three U.S. regions (Fig. 1) are averaged for 80-m  $u$ ,  $v$ , and total wind speed. The annually averaged  $u$  and  $v$  components have similar values in the range of  $3\text{--}3.3 \text{ m s}^{-1}$  in the western region (triangles in Figs. 6a and 6b), with both showing a steady positive trend from 1979 to 2009 (regression lines in Figs. 6a and 6b) with  $u$  at  $0.06 \text{ m s}^{-1} (10 \text{ yr})^{-1}$  and  $v$  at  $0.07 \text{ m s}^{-1} (10 \text{ yr})^{-1}$ . As a result, the corresponding total wind shows a positive trend of  $0.1 \text{ m s}^{-1} (10 \text{ yr})^{-1}$  (Fig. 6c). Relative to the western region, the central region shows larger values of  $u$  in the range of  $3.7\text{--}4 \text{ m s}^{-1}$  (Fig. 6d), and  $v$  in the range of  $3.3\text{--}3.5 \text{ m s}^{-1}$  (Fig. 6e), as well as larger total wind values in the range of  $5.5\text{--}6.0 \text{ m s}^{-1}$  (Fig. 6f). These values are averaged annually. The trends in  $u$ ,  $v$ , and total wind over the central United States during 1979–2009 are, respectively,  $0.08$ ,  $0.08$ , and  $0.12 \text{ m s}^{-1} (10 \text{ yr})^{-1}$  at the 95% significance level, and all are larger than their counterparts for the western region by 20%–30%. For the eastern region of the United States,  $u$  (Fig. 6g),  $v$  (Fig. 6h), and total wind (Fig. 6i) all show virtually no changes in the range of their values, but their

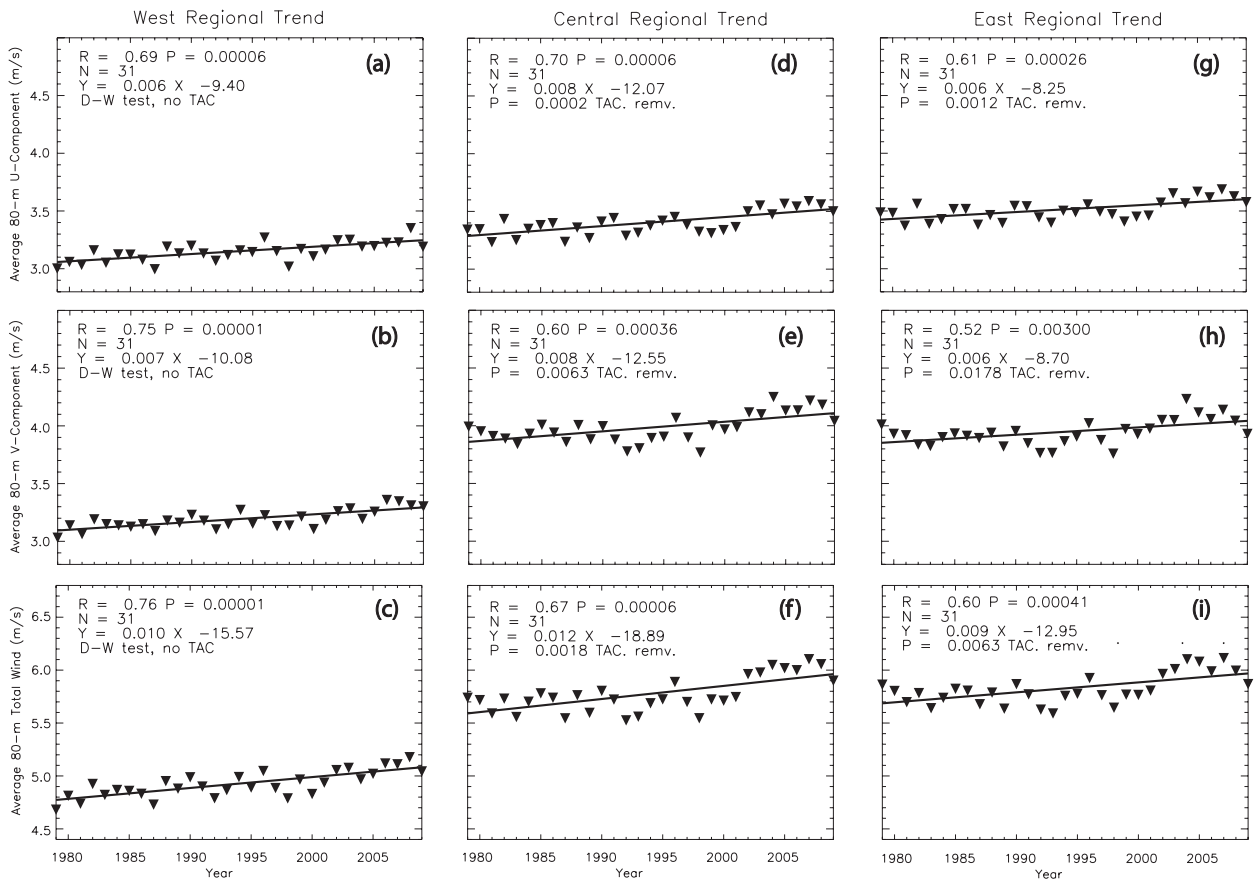


FIG. 6. The 1979–2009 time series of annually averaged (top) 80-m  $u$  wind, (middle) 80-m  $v$  wind, and (bottom) 80-m total wind speed over three U.S. regions: (left) west, (center) central, and (right) east. The definitions of regions follow Fig. 1. In each panel, the solid line shows the best linear fits of the variation of variables ( $y$  axis) with time ( $x$  axis) during 1979–2009. The statistics for the linear fit, based upon the OLS, including the correlation coefficient  $R$ , number of data samples  $N$ , the equation of the fit, and the statistical significance  $P$ , are also shown. Also shown in the fourth line (from the top) of the statistics in each panel is either the pass of the DW test for temporal autocorrelation in the corresponding time series data (D–W test, no TAC) or the final  $P$  after removing the temporal autocorrelation (denoted as TAC. remv.) on the basis of the CO method.

corresponding trends are generally smaller by 20%–30% (when compared with their counterparts in the central United States). Overall, Fig. 6 again shows that stronger winds combined with a relatively uniform topography make the central United States a relatively appealing place for the development of wind power plants in the United States, although the electrical transmission capacity, the density and distance of population and urban centers, and local and regional policies are other important factors that should be considered.

## 5. Interpretation of results and discussion of uncertainties

On the basis of section 4, we conclude that significant positive trends in the wind speed (at 10 and 80 m above

the surface) are evident over much of the continental United States. This result is in contrast to previous studies that used near-surface (10 m) wind speeds from *ground-based observations* and found slight declines in wind trends (Pryor et al. 2007; Vautard et al. 2010) but, to a large extent, does support the positive trend found in the global reanalysis data (Pryor and Ledolter 2010). In addition, our analysis also supports the findings of Vautard et al. (2010) that the trend in 80-m wind speed is larger than the trend at 10 m, reflecting the influence of the increasing trend in wind in the upper part of the boundary layer. Inconsistency between observations and model results of wind trends is thought to be due to deficiencies and/or missing key processes (such as land-use changes) in the models (Pryor and Ledolter 2010; Vautard et al. 2010), while the increase in surface roughness (due to tree growth and urban development)

might also be a major source of artificial error in the surface observations (Vautard et al. 2010; DeGaetano 1998). Hence, interpretation of the results in this study should be done cautiously and with consideration of at least the following caveats and challenges: 1) the explanation of the physical mechanisms for the wind trends and 2) the fidelity of the wind data in the NARR.

A thorough investigation of the mechanisms for the wind trend revealed in this study will be part of future work. Our analysis of the trend in  $u$  and  $v$ , which has not been conducted in past research, is intriguing enough to hypothesize that the wind trend found here is linked in part to past reported climate changes, such as the strengthening of the low-level jet, the subtropical highs, and the zonal winds. From climate-model simulations, Kushner et al. (2001) showed that, within a warming climate, the upper-level zonal wind and eddy kinetic energy are likely to increase in response to the thermal wind balance from tropospheric warming and stratospheric cooling (Lorenz and DeWeaver 2007). Furthermore, Lu et al. (2008) showed in their modeling studies that, in response to global warming, the mid- to low-level subtropical air temperature gradient decreases, the zonal mean midlatitude westerlies and tropospheric zonal jet shift poleward, and the subtropical highs move poleward. Their proposed mechanisms further support Lorenz and DeWeaver (2007) in suggesting that the change in the height of the tropopause may also be responsible for the poleward shifts in the tropospheric jets and synoptic-scale storm tracks, leaving much of the Great Plains susceptible to intensified subtropical (Bermuda) highs that favor more-frequent southerly and westerly low-level jet formation (Song et al. 2005). In fact, analysis of the NARR indicates that the core of the low-level jet over the Great Plains has strengthened/expanded by 38% from 1979 to 2003 (Weaver and Nigam 2008). These modeling-based studies and analyses all support and can also explain our major findings: 1) The trend in southerly wind (and to some extent the trend in westerly wind) is distinct over the Southeast, including Arkansas, Texas, Oklahoma, and Louisiana during the winter and spring seasons because of the poleward shift of the subtropical Bermuda high and strengthening of the low-level jet emanating from Gulf of Mexico (Fig. 5). 2) The trend in westerly wind is distinct in the northern states bordering Canada in all seasons (Fig. 5) because of the poleward shift and strengthening (expansion) of the tropospheric midlatitude zonal jets. 3) The trend in wind speed is large over the high plains because of an increase in midlatitude cyclone intensity (Lambert 1995; McCabe et al. 2001), specifically cyclones that develop off of the leeward side of the Rocky Mountains. For the future,

model simulations contributing to the Intergovernmental Panel on Climate Change report all showed continuous warming, but different global model simulations may not give a consistent trend in wind speed (Pryor and Barthelmie 2011), and a downscaling technique is needed to study the trend at the regional scale (Pryor et al. 2005).

The results presented in section 4 are subject to any deficiencies in the NARR dataset, because this study uses only NARR data. Past investigations show that the surface (10 m) wind data in the NARR have a much better accuracy than other global reanalysis datasets but also have a slightly negative bias ( $<0.5 \text{ m s}^{-1}$  when compared with surface observations) in both summer and winter (Mesinger et al. 2006). Pryor et al. (2009) showed that 10-m wind in the NARR has different (and sometime opposite) trends relative to those from ground-based observations, although the ground-based data themselves are subject to uncertainties and errors from instrumentation (Pryor et al. 2009). At the regional scale, Li et al. (2010) compared their 80-m wind estimate (assuming a linear profile of the wind) with those from radiosonde data and found that the standard-deviation error in their estimation is  $0.28 \text{ m s}^{-1}$  with a correlation coefficient of generally larger than or close to 0.8. No evidence has been shown that the bias in the NARR wind data affects the trend analysis (Pryor et al. 2009). More analyses with other modeled data and evaluations of these data with well-calibrated observed wind data certainly are warranted (Pryor and Barthelmie 2011).

## 6. Implication for the trend in wind power potential

Because wind power is proportional to the wind speed cubed, the trend in larger wind speed has a disproportionately larger impact on the trend in wind power than the does the trend for smaller wind speed. Archer and Jacobson (2003) assess the wind resource in the United States for wind speeds of no less than  $3 \text{ m s}^{-1}$  because many turbines may not be able to produce power at wind speeds that are lower than this threshold. In this paper we compute the trends for both annual averages of 80-m wind speed  $\geq 3 \text{ m s}^{-1}$  and the 90th quantile of the annual wind speeds; the latter is used more often in recent assessments of wind power trends [see review in Pryor and Barthelmie (2011)].

We found that the geographical distribution of both trends is similar except that the trend for annual averages of wind speed  $\geq 3 \text{ m s}^{-1}$  is  $\sim 20\%–30\%$  smaller than that of the 90th quantile of the annual wind speed; the latter is shown in Fig. 7a together with the trends for the 90th quantile of horizontal wind speed (absolute value of  $u$ ) and meridional wind speed (absolute value of  $v$ ) in

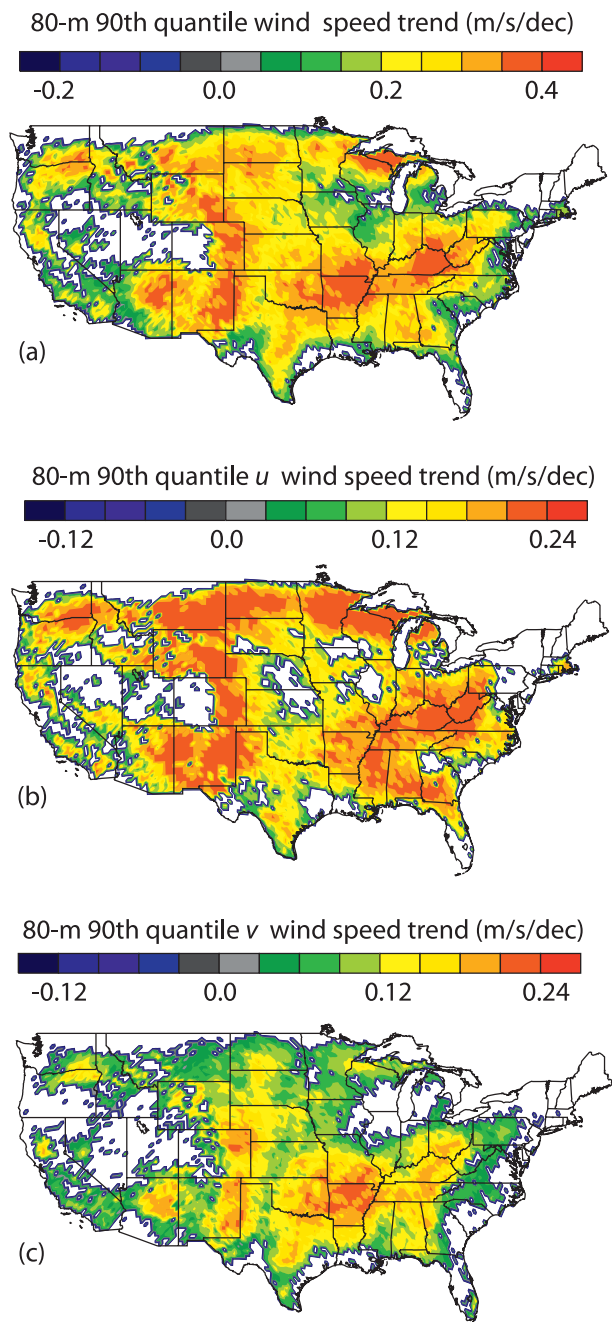


FIG. 7. (a) Trend in the 90th percentile of annual wind speed during 1979–2009. (b),(c) As in (a), but for the 90th percentile of the horizontal and meridional wind speeds, respectively. Areas in white indicate the regions that either are covered by a water surface or have statistically insignificant trends.

Figs. 7b and 7c, respectively. The trends for the 90th quantile of the annual wind speed (Fig. 7a) are generally 40%–50% larger than, but with similar geographical distributions to, its counterpart for annual averages of 80-m wind speed (Fig. 4a). Larger positive trends [up

to  $0.4 \text{ m s}^{-1} (10 \text{ yr})^{-1}$ ] are found over states in the Southeast (including Arkansas, Tennessee, Kentucky, Alabama, and Georgia), in the northern border states (including Minnesota, North Dakota, and Montana), and in the west-central United States (including northwestern Texas, New Mexico, eastern Colorado, and Wyoming). Similar geographical distributions are found for 90th-quantile trends in horizontal (Fig. 7b) and meridional wind speeds (Fig. 7c), with the following exceptions: 1) trends over the northern states are dominated by the horizontal winds, 2) horizontal wind trends over the southeastern United States are larger than (if not equal to) that of the meridional winds, and 3) trends in horizontal winds over states in the west-central United States are of a similar magnitude to (although slightly larger than) that of the meridional wind speed.

Overall, the analysis of trend for the 90th percentile of wind speed reveals the same pattern that we find in the analysis of the trend for the annual wind speed—both showing increases in wind power resources from 1979 to 2009 over the majority of the contiguous United States (except in the Northeast and Intermountain West regions), with larger trends over the northern border regions, the high plains, and the southeastern United States.

## 7. Summary

This study has provided a statistical assessment of the linear trends of wind at a common hub height of 80 m using the NARR gridded dataset. Linear trends in 80-m wind speed from 1979 to 2009 in each NARR model grid box over the contiguous United States are analyzed. One emphasis of this work focuses on the estimates of the  $u$  and  $v$  components of wind at 80 m so that the trend in wind speed at 80 m can be better interpreted within the context of the reported changes of various synoptic systems (low-level jet over the Great Plains, tropospheric zonal jet, subtropical high, etc.). Critical to our estimate of the wind at 80 m is the location of two altitudes that are directly below and above 80 m and have available wind data from the NARR. This is done through the use of the hydrostatic equation while accounting for terrain and air-density variations.

Over the majority of the United States, it is found that high wind speed and the trend in wind speed are evident over the west-central section of the country, representing the regions with the largest wind resources and the most potential for commercial development. This finding is consistent with that of Archer and Jacobson (2003), although other factors such as transmission-line proximity and government policies may also play an important role in the commercial development of wind

entities. Trends are found to be generally positive from 1979 to 2009 for all wind variables studied. The trends at the surface are relatively small, however. In contrast, trends at 80 m are mostly positive with large values in the Southeast, the west-central states, and the northern border states. Our results contrast with previous works that show negative trends at the surface using observational stations (while citing significant errors) but is consistent with positive trends higher in the boundary layer that were found in Li et al. (2010) and Vautard et al. (2010).

Seasonal analyses show that spring and winter are the two seasons that contribute the most to the increasing trend in annually averaged wind power, whereas summer contributes the least. The positive trend in southerly wind exists over the southeastern United States in all seasons and has distinctly larger values in spring and winter, which may reflect the strengthening of the subtropical highs in response to climate change (Lorenz and DeWeaver 2007). Furthermore, the strong positive trend in southerly wind is also found in all seasons in the high plains, suggesting the role of the strengthening low-level jet over the southern plains and the Gulf Coast region (Lorenz and DeWeaver 2007). In contrast, the large positive trend in westerly winds is found in all seasons over the northern states along the Canadian border, which can be interpreted as the result of the enhancement and polar shift of midlatitude zonal jets (Lu et al. 2008). Further modeling studies are needed to evaluate our proposed link between the wind trend and climate change, and more observational-based analyses are required to validate our trend analysis and to resolve differences among different studies.

*Acknowledgments.* This manuscript is part of author Holt's master's thesis. The authors thank Drs. Clinton Rowe and Adam Houston at the University of Nebraska—Lincoln for their constructive comments, Dr. David Watkins for his advice and support, and Tina Gray and Wendi Fletcher for their logistical help. The authors are also thankful for two anonymous reviews whose comments were valuable for shaping and improving the manuscript. Author Holt is grateful to the following people who helped him perform this work during his graduate studies: Dr. Mark Anderson, Dr. Song Feng, Dave Peterson, George Limpert, Richard Xu, and Michael Veres. He also thanks the Department of Earth and Atmospheric Science for funding his teaching-assistant position, which allowed him to perform this work. Last, author Holt thanks his parents Mike and June Holt for their continuous moral support over the years.

## REFERENCES

- Archer, C. L., and M. Z. Jacobson, 2003: Spatial and temporal distributions of U.S. winds and wind power at 80 m derived from measurements. *J. Geophys. Res.*, **108**, 4289, doi:10.1029/2002JD002076.
- , and —, 2005: Evaluation of global wind power. *J. Geophys. Res.*, **110**, D12110, doi:10.1029/2004JD005462.
- Arya, P. S., 2001: *Introduction to Micrometeorology*. 2nd ed. Academic Press, 307 pp.
- AWEA, cited 2009: Wind power outlook: 2009. American Wind Energy Association. [Available online at [http://archive.awea.org/pubs/documents/Outlook\\_2009.pdf](http://archive.awea.org/pubs/documents/Outlook_2009.pdf).]
- Barthelmie, R. J., 1999: The effects of atmospheric stability on coastal wind climates. *Meteor. Appl.*, **6**, 39–47.
- Capps, S. B., and C. S. Zender, 2009: Global ocean wind power sensitivity to surface layer stability. *Geophys. Res. Lett.*, **36**, L09801, doi:10.1029/2008GL037063.
- Chuang, H.-Y., G. Manikin, and R. Treadon, 2001: The NCEP Eta Model post processor: A documentation. NCEP Office Note 438, 52 pp. [Available online at <http://www.emc.ncep.noaa.gov/mmb/papers/chuang/1/OF438.html>.]
- DeGaetano, A. T., 1998: Identification and implications of biases in U.S. surface wind observation, archival, and summarization methods. *Theor. Appl. Climatol.*, **60**, 151–162, doi:10.1007/s007040050040.
- Ebisuzaki, W., J. Alpert, J. Wang, D. Jovic, and P. Shafran, 2004: North American Regional Reanalysis: End user access to large data sets. Preprints, *20th Int. Conf. on Interactive Information and Processing Systems (IIPS) for Meteorology, Oceanography, and Hydrology*, Seattle, WA, Amer. Meteor. Soc., 8.2. [Available online at <http://ams.confex.com/ams/pdfpapers/73708.pdf>.]
- Elliot, D. L., C. G. Holladay, W. R. Barchet, H. P. Foote, and W. F. Sandusky, 1986: Wind Power Resource Atlas of the United States., National Renewable Power Laboratory. Solar Technical Information Program Rep., 327 pp. [Available online at <http://rredc.nrel.gov/wind/pubs/atlas/>.]
- Foltz, C. S., S. A. Lack, N. I. Fox, A. R. Lupo, and J. R. Hasheider, 2007: Advancing renewables in the Midwest. *Bull. Amer. Meteor. Soc.*, **88**, 1097–1099.
- Griffin, B. J., K. E. Kohfeld, A. B. Cooper, and G. Boenisch, 2010: Importance of location for describing typical and extreme wind speed behavior. *Geophys. Res. Lett.*, **37**, L22804, doi:10.1029/2010GL045052.
- GWEC, cited 2011: Global wind statistics 2010. Global Wind Energy Council. [Available online at [http://www.gwec.net/fileadmin/documents/Publications/GWEC\\_PRstats\\_02-02-2011\\_final.pdf](http://www.gwec.net/fileadmin/documents/Publications/GWEC_PRstats_02-02-2011_final.pdf).]
- Hundecha, Y., A. St-Hilaire, T. B. M. J. Ouarda, S. El Adlouni, and P. Gachon, 2008: A nonstationary extreme value analysis for the assessment of changes extreme annual wind speed over the Gulf of St. Lawrence. *J. Appl. Meteor. Climatol.*, **47**, 2745–2759.
- Janjić, Z. I., 1994: The step-mountain eta coordinate model: Further developments of the convection, viscous sublayer, and turbulence closure schemes. *Mon. Wea. Rev.*, **122**, 927–945.
- Klink, K., 1999: Trends in mean monthly maximum and minimum surface wind speeds in the coterminous United States, 1961 to 1990. *Climate Res.*, **13**, 193–205.
- , 2007: Atmospheric circulation effects on wind speed variability at turbine height. *J. Appl. Meteor. Climatol.*, **46**, 445–456.
- Kushner, P. J., I. M. Held, and T. L. Delworth, 2001: Southern Hemisphere atmospheric response to global warming. *J. Climate*, **14**, 2238–2249.

- Lambert, S. J., 1995: The effect of enhanced greenhouse warming on winter cyclone frequencies and strengths. *J. Climate*, **8**, 1447–1452.
- Li, X., S. Zhong, X. Bian, and W. E. Heilman, 2010: Climate and climate variability of the wind power resources in the Great Lakes region of the United States. *J. Geophys. Res.*, **115**, D18107, doi:10.1029/2009JD013415.
- Lobocki, L., 1993: A procedure for the derivation of surface-layer bulk relationships from simplified second-order closure models. *J. Appl. Meteor.*, **32**, 126–138.
- Lorenz, D. J., and E. T. DeWeaver, 2007: Tropopause height and zonal wind response to global warming in the IPCC scenario integrations. *J. Geophys. Res.*, **112**, D10119, doi:10.1029/2006JD008087.
- Lu, J., G. Chen, and D. M. W. Frierson, 2008: Response of the zonal mean atmospheric circulation to El Niño versus global warming. *J. Climate*, **21**, 5835–5851.
- Lu, X., M. McElroy, and J. Kiviluoma, 2009: Global potential for wind generated electricity. *Proc. Natl. Acad. Sci. USA*, **106**, 10 933–10 938.
- McCabe, G. J., M. P. Clark, and M. C. Serreze, 2001: Trends in Northern Hemisphere surface cyclone frequency and intensity. *J. Climate*, **14**, 2763–2768.
- McElroy, M. B., X. Lu, C. P. Nielsen, and Y. Wang, 2009: Potential for wind-generated electricity in China. *Science*, **325**, 1378–1380.
- McVicar, T. R., L. Li, T. G. Van Niel, M. F. Hutchinson, X. Mu, and Z. Liu, 2005: Spatially distributing 21 years of monthly hydrometeorological data in China: Spatio-temporal analysis of FAO-56 crop reference evapotranspiration and pan evaporation in the context of climate change. CSIRO Land and Water Tech. Rep. 8/05, 324 pp.
- , T. G. Van Niel, L. Li, M. L. Roderick, D. P. Rayner, L. Ricciardulli, and R. J. Donohue, 2008: Wind speed climatology and trends for Australia, 1975–2006: Capturing the stilling phenomenon and comparison with near-surface reanalysis output. *Geophys. Res. Lett.*, **35**, L20403, doi:10.1029/2008GL035627.
- Mellor, G. L., and T. Yamada, 1974: A hierarchy of turbulence closure models for planetary boundary layers. *J. Atmos. Sci.*, **31**, 1791–1806.
- Mesinger, F., 2010: Several PBL parameterization lessons arrived at running an NWP model. *Earth Environ. Sci.*, **13**, 012005, doi:10.1088/1755-1315/13/1/012005.
- , and Coauthors, 2006: North American Regional Reanalysis. *Bull. Amer. Meteor. Soc.*, **87**, 343–360.
- Metz, B., O. R. Davidson, P. R. Bosch, R. Dave, and L. A. Meyer, Eds., 2007: *Climate Change 2007: Mitigation of Climate Change*. Cambridge University Press, 808 pp.
- Peterson, E. W., and J. P. Hennessey, 1978: On the use of power laws for estimates of wind power potential. *J. Appl. Meteor.*, **17**, 390–394.
- Pirazzoli, P. A., and A. Tomasin, 2003: Recent near-surface wind changes in the central Mediterranean and Adriatic areas. *Int. J. Climatol.*, **23**, 963–973.
- Pryor, S. C., and J. Ledolter, 2010: Addendum to “Wind speed trends over the contiguous United States.” *J. Geophys. Res.*, **115**, D10103, doi:10.1029/2009JD013281.
- , and R. J. Barthelmie, 2011: Assessing climate change impacts on the near term stability of the wind energy resource over the United States. *Proc. Natl. Acad. Sci. USA*, **108**, 8167–8171.
- , J. T. Schoof, and R. J. Barthelmie, 2005: Empirical downscaling of wind speed probability distributions. *J. Geophys. Res.*, **110**, D19109, doi:10.1029/2005JD005899.
- , R. J. Barthelmie, and E. S. Riley, 2007: Historical evolution of wind climates in the USA. *J. Phys. Conf. Ser.*, **75**, 012065, doi:10.1088/1742-6596/75/1/012065.
- , and Coauthors, 2009: Wind speed trends over the contiguous United States. *J. Geophys. Res.*, **114**, D14105, doi:10.1029/2008JD011416.
- Ray, M. L., A. L. Rogers, and J. G. McGowan, 2006: Analysis of wind shear models and trends in different terrains. *Windpower 2005 Conf.*, Pittsburgh, PA, Amer. Wind Energy Association. [Available online at [http://www.ceere.org/rerl/publications/published/2006/AWEA\\_202006\\_20Wind\\_20Shear.pdf](http://www.ceere.org/rerl/publications/published/2006/AWEA_202006_20Wind_20Shear.pdf).]
- Robeson, S. M., and K. A. Shein, 1997: Spatial coherence and decay of wind speed and power in the north-central United States. *Phys. Geogr.*, **18**, 479–495.
- Roderick, M. L., L. D. Rotstain, G. D. Farquhar, and M. T. Hobbins, 2007: On the attribution of changing pan evaporation. *Geophys. Res. Lett.*, **34**, L17403, doi:10.1029/2007GL031166.
- Song, J., K. Liao, R. L. Coulter, and B. M. Lesht, 2005: Climatology of the low-level jet at the Southern Great Plains Atmospheric Boundary Layer Experiments site. *J. Appl. Meteor.*, **44**, 1593–1606.
- Thejll, P., and T. Schmith, 2005: Limitations on regression analysis due to serially correlated residuals: Application to climate reconstruction from proxies. *J. Geophys. Res.*, **110**, D18103, doi:10.1029/2005JD005895.
- Tuller, S. E., 2004: Measured wind speed trends on the west coast of Canada. *Int. J. Climatol.*, **24**, 1359–1374.
- Vautard, R., J. Cattiaux, P. Yiou, J.-N. Thepaut, and P. Ciais, 2010: Northern Hemisphere atmospheric stilling partly due to an increase in surface roughness. *Nat. Geosci.*, **3**, 756–761, doi:10.1038/NGEO979.
- Weaver, J. S., and S. Nigam, 2008: Variability of the Great Plains low-level jet: Large-scale circulation context and hydroclimate impacts. *J. Climate*, **21**, 1532–1551.
- Wilks, D. S., 2006: *Statistical Methods in the Atmospheric Sciences*. 2nd ed., Academic Press, 627 pp.
- Xu, C., L. Gong, T. Jiang, D. Chen, and V. P. Singh, 2006a: Analysis of spatial distribution and temporal trend of reference evapotranspiration and pan evaporation in Changjiang (Yangtze River) catchment. *J. Hydrol.*, **327**, 81–93.
- Xu, M., C.-P. Chang, C. Fu, Y. Qi, A. Robock, D. Robinson, and H. Zhang, 2006b: Steady decline of East Asian monsoon winds, 1969–2000: Evidence from direct ground measurements of wind speed. *J. Geophys. Res.*, **111**, D24111, doi:10.1029/2006JD007337.